Alterations of Chromatin Accessibility of Human Mesenchymal Stem Cells During Early Differentiation Stage Toward Osteoblasts and Adipocyte

Jianyun Liu
Jiujiang University
Lijun Gan
Jiujiang University
Baichen Ma
Jiujiang University
Shan He
Jiujiang University
Ping Wu
Jiujiang University
Huiming Li
Jiujiang University
Jianjun Xiong (xiongjj1975@163.com)
Jiujiang University

Research Article

Keywords: MSC, ATAC-seq, RNA-seq, Adipogenic, Osteogenic

Posted Date: November 12th, 2021

DOI: https://doi.org/10.21203/rs.3.rs-1055172/v1

Abstract

Although differential expression of genes is apparent during the adipogenic/osteogenic differentiation of marrow mesenchymal stem cells (MSCs), it is not known whether this is associated with changes in chromosomal structure. In this study, we used ATAC-sequencing technology to observe variations in chromatin assembly during the early stages of MSC differentiation. This showed significant changes in the number and distribution of chromosome accessibility at different time points of adipogenic/osteogenic differentiation. Sequencing of differential peaks indicated alterations in transcription factor motifs involved in MSC differentiation. Gene Ontology (GO) and pathway analysis indicated that changes in biological function resulted from the alterations in chromatin accessibility. We then integrated ATAC-seq and RNA-seq and found that only a small proportion of the overlapped genes were screened out from ATAC-seq and RNA-seq overlapping. Through GO and pathway analysis of these overlapped genes, we not only observed some known biological functions related to adipogenic/osteogenic differentiation but also noticed some unusual biological clustering during MSC differentiation. In summary, our work not only presents the landscape of chromatin accessibility of MSC during differentiation but also helps to further our understanding of the underlying mechanisms of gene expression in these processes.

1. Introduction

Osteoporosis, involving reductions in bone mass, microstructure reduction, and increased bone fragility and fracture, is a global public health problem[1]. According to the classical view, the occurrence of osteoporosis is related to increased osteoclast production and activity, resulting in the loss of bone mass and the decline of bone quality[2]. Recent studies have confirmed that an imbalance in the differentiation of bone marrow-derived mesenchymal stem cells (MSCs) into osteoblasts (OBs) and adipocytes (ADs) is a key factor in osteoporosis [3, 4].

MSCs are characterized by strong self-renewal abilities and can differentiate into different cell types[5]. The direction of differentiation is reflective of fundamental alterations in the gene expression pattern promoting the formation of adipocytes or osteoblasts. In *in vitro* culture, adipogenic/osteogenic inducers are commonly used to induce MSCs directional differentiation. After 14-21 days of treatment, a significant alteration in gene expression was observed to promote the differential differentiation and maturation of MSCs into adipocytes or osteoblasts[6, 7].

In eukaryotes, modulation of gene expression may occur at the levels of transcription, post-transcriptional regulation, translation, and post-translational modification. Due to the rapid development and application of next-generation sequencing, numerous investigations into the transcriptomes of adipocytes or osteoblasts derived from MSCs have been undertaken, providing a suitable basis for studying the mechanism of MSC differentiation [8–11]. However, the transcriptional activation mechanisms of many genes are still unclear.

Epigenetics dynamically regulates transcription and plays a crucial role in cellular functioning[12]. Assays for transposase accessible chromatin using sequencing (ATAC-seq) is an epigenetic technique used to identify the accessibility of chromatin [13]. Obtaining the location of the accessible region and the active regulatory sequence on chromatin helps to infer the possible binding of transcription factors and their actions in the whole genome [14]. Here, we aimed to investigate variations in chromatin accessibility in the early stage of MSC differentiation, integrating this with RNA-seq. This will provide a new entry point for exploring MSC differentiation and will help to identify more effective target genes for controlling osteogenic/adipogenic directional differentiation.

2. Materials And Methods

2.1. hMSCs culture

Two strains of human primary cultured MSCs were acquired from the respective bone marrow of a 21-year-old and a 22-year-old healthy male. The project was approved by the ethics committee of Jiujiang University Subsidiary Hospital. The isolation, characterization, culture, and storage of the MSCs were conducted as previously described [15]. For adipogenic differentiation assays, sixth-generation MSCs were incubated with a stimulation cocktail of minimum essential medium (MEM) α containing 10% fetal bovine serum (FBS), 1.0 μM dexamethasone, 0.5 mM 3-isobutyl-1-methylxanthine, and 0.01 mg/ml insulin. Adipogenesis was confirmed by staining with Oil Red O after 14 days. For osteoblast differentiation, MSCs were incubated in MEM α containing 10% FBS, 100 mM dexamethasone, 10 mM sodium glycerophosphate, and 50 ng/ml vitamin C. Osteogenesis was confirmed by Alizarin Red staining after 14 days.

2.2. Transposition reaction and PCR amplification

After adipogenic and osteogenic induction of MSCs, cells from each group were harvested and digested into single-cell suspensions. For the transposition reaction, 5×10^4cells from each group were centrifuged for 5 min at 500 × g at 4°C and the supernatant was discarded. After washing with cold phosphate-buffered saline (PBS), the cells were resuspended by gentle pipetting in 50 μl of chilled lysis buffer (10 mM Tris-HCl, pH 7.4, 10 mM NaCl, 3 mM MgCl2, 0.1% IGEPAL CA-630) and immediately centrifuged for 10 min as above. The precipitate was resuspended in the transposition reaction mixture from the Nextera kit (Illumina, San Diego, CA, USA) consisting of 25 μl TD (2× reaction buffer from the kit), 2.5 μl TDE1 (Nextera Tn5 Transposase from the kit), and 22.5 μl nuclease-free H_2O. The mixture was then incubated at 37°C for 30 min. The reaction products were then purified using a Qiagen MinElute PCR Purification Kit (Qiagen, Hilden, Germany) and eluted in 10 μl elution buffer. Before

amplifying the transposed DNA fragments, the following reagents were mixed: 10 μl transposed DNA, 10 μl nuclease-free H_2O, 2.5 μl of 25 μM PCR Primer 1, 2.5 μl of 25 μM Barcoded PCR Primer 2, and 25 μl NEBNext High-Fidelity 2× PCR Master Mix in a 0.2 ml PCR tube. The thermal cycle was as follows: 72°C for 5 min, 1 cycle; 98°C for 30 sec; 98°C for 10 sec, 5 cycles; 63°C for 30 sec; 2°C for 2 min. The amplified products were purified by the Qiagen MinElute PCR Purification Kit.

2.3. Sequencing and data analysis

ATAC-sequencing was performed by Jiayin Biotechnology Ltd (Shanghai, China). Fast QC software was used for the quality control of sequencing data. Raw data from the machine were processed by the connector. BWA software compared the clean data to the reference genome hg38_genecode. The BAM file obtained after comparison and analysis was used as the input file, and the peaks were called using MACS2 software, with a filtering threshold of $Q < 0.05$. Each peak region extended 200 bp from the 5' end to the 3' end to extract the DNA sequence. The motif was predicted using Homer software and the predicted motif was matched with the motif data in the database (Homer and Jaspar), and known motifs and corresponding transcription factors were screened out. Deeptools software was used to analyze the signal distribution near the gene. Gene Ontology (GO) was used to elucidate the biological processes (BPs) of genes associated with the accessible chromatin regions. The Kyoto Encyclopedia of Genes and Genomes (KEGG) database was used to analyze enriched pathways of the genes adjacent to the peaks.

2.4. RNA-seq

To relate chromatin accessibility to mRNA expression, we performed RNA-seq on the same batch of cells used for ATAC-seq. Total RNA was extracted with the TRIzol reagent (Invitrogen) and was used for library construction with the NEBNext Ultra Directional RNA Library Prep Kit, following the manufacturer's instructions. RNA-seq sequencing was performed by NovelBio Bio-Pharm Technology Co., Ltd (Shanghai, China) using commercially available protocols.

2.5. Combination of the ATAC-seq and RNA-seq data

To integrate the ATAC-seq and RNA-seq data, genes observed to be downregulated in both groups were overlapped for further analysis. Upregulated genes from both groups were also overlapped.

2.6. Real-time PCR verification

The RNA-seq data were verified using qRT-PCR. Specifically, the sequencing data of 12 genes identified as being closely associated with adipogenesis or osteogenesis were analyzed using a 7500 Real-Time PCR System (ABI, Foster, CA, USA). The primers used are listed in Supplementary Table 1. First-strand cDNA synthesis was performed using a cDNA synthesis kit (Toyobo, Osaka, Japan), and PCR used the SYBR Green Realtime PCR Master Mix (Toyobo) at 94°C for 5 min, 58°C for 34 s, and a final extension at 72°C with 30 cycles. β-actin was used as the internal control.

3. Results

3.1. Landscape of chromatin accessibility

Sixth-generation primary hMSCs were stimulated by adipogenic or osteogenic inducers, and the differentiated morphology was confirmed by Oil Red O staining and Alizarin Red staining, respectively (Figure 1A). Based on the successful differentiation, we harvested cells at specified times during differentiation for ATAC-seq and RNA-seq analysis (Figure 1B).

We first conducted ATAC-seq. Data quality checking showed that the rate of effective reads in each group was higher than 90% (Table 1), indicating the reliability of the sequencing. The peak numbers in each group calculated by MACS2 software are listed in Table1. Notably, the number of accessible chromatin regions decreased significantly in the adipogenic AD3 group, and gradually recovered in the AD5 and AD7 groups. In contrast, there were minimal changes in the numbers of accessible chromatin regions in the osteogenic OB3 and OB5 groups, although a significant reduction was seen in the OB7 group. Analysis of the read distributions using Deeptools showed that the majority of the read signals in each group were concentrated near the transcriptional start sites (TSS), and were also concentrated near the centers of peaks (Supplementary Figure 1A and B), indicating the reliability of the sequencing. The accessible peaks in each group were widely distributed throughout the genome (Figure 1C). Specifically, the proportions of peaks in the intronic and intergenic regions were relatively high (approximately 80%), while the percentages of peaks in the promoter regions fluctuated between 10% and 20% in all groups. In adipogenic differentiation, the highest proportion of accessible chromatin regions located in the promoter regions was seen in the AD3 group (17.63%), while the number of read signals was the lowest (68 327). Conversely, in the osteoblast differentiation groups, the highest percentage of accessible chromatin regions located in the promoters was in the OB7 group (15.98%), which also showed the lowest peak number (68 216).

Table.1 Summary of ATAC-seq, read mapping, motif, and peak calling results

	MSC	AD3	AD5	AD7	OB3	OB5	OB7
Mapped reads	144722564	142125644	138602489	199777605	149649854	146697518	144753928
Mapped rate	99%	98.1%	98.5%	96.8%	96.7%	91.8%	97.5%
Peak numbers	110 369	68 327	99 362	77 712	113785	110267	68216
Motif binding	270998	150410	220839	152472	295624	275090	98411
Motif types	577	555	562	533	570	560	522
Gene numbers*	19264	20193	19227	19936	19348	19023	18825
* RNA-seq results							

3.2. Motif analysis

We used HOMER to identify transcription factor-binding motifs enriched in the accessible chromatin regions. The total numbers and types of motifs showed minimal variation between the different groups (Table 1). The top 10 major motifs identified in each group are listed in Supplementary Table 1, with most of them, such as fra1, fra2, ATF3, junB, BATF, and AP-1, belonging to the basic leucine zipper (bZIP) transcription factor family. We next examined alterations in these motifs during the differentiation process. Using MSC as the control group, the major changes in the motifs in the different groups are shown in Table 2. Specifically, during adipogenic differentiation, the top motifs identified in the AD3 and AD5 groups remained similar, specifically, motifs belonging to the CEBP, NFIL3, and HLF families, while in AD7 group, the most common motifs belonged to the TEAD family. Interestingly, the number of RUNX family motifs began to increase in the AD5 group. On the other hand, during osteogenic differentiation, the transcription factor families showing the greatest increase were TEAD and RUNX in the OB3 and OB5 groups, changing to CEBP, NFIL3, and HLF in the OB7 group. Interestingly, no clear pattern was discernable for the decreased motifs.

Since PPARγ and RUNX2 are considered to be key regulatory transcription factors in adipogenic and osteogenic differentiation, respectively, we specifically tracked their dynamic enrichment. As expected, enrichment of the PPARγ motif was increased in the AD3 and AD5 groups but diminished in the AD7 group. Similarly, enrichment of RUNX was enhanced in the OB3 and OB5 groups but decreased in the OB7 group (Supplementary Figure 2).

Table 2
The 10 top-ranking motifs that changed with differentiation in each group.

	AD3 vs. MSC		AD5 vs. MSC		AD7 vs. MSC		OB3 vs. MSC		OB5 vs. MSC		OB7 vs. MSC	
Rank	up	down	up	down	up	down	up	down	up	down	up	down
1	CEBP	Atf3	CEBP	Fra1	TEAD3	Fra1	TEAD3	Fra1	RUNX1	Atf3	CEBP	Fra1
2	NFIL3	Fra1	CEBP:AP1	Atf3	TEAD1	Atf3	TEAD1	Atf3	TEAD1	Fra1	EBF2	Atf3
3	HLF	BATF	HLF	BATF	TEAD4	BATF	TEAD4	AP-1	TEAD3	AP-1	NFIL3	BATF
4	EBF2	AP-1	NFIL3	Fra2	TEAD	AP-1	RUNX	BATF	TEAD4	BATF	HLF	Fra2
5	CEBP:AP1	JunB	RUNX1	AP-1	CEBP	Fra2	RUNX1	JunB	RUNX2	JunB	CEBP:AP1	JunB
6	NF1	Fra2	EBF2	JunB	RUNX2	JunB	RUNX2	Fra2	RUNX-AML	Fra2	NF1	AP-1
7	Atf4	Fosl2	RUNX2	Fosl2	RUNX1	Fosl2	CEBP	Fosl2	TEAD2	Fosl2	EBF1	Fosl2
8	EBF1	Jun-AP1	RUNX-AML	Jun-AP1	NF1	Jun-AP1	TEAD2	Jun-AP1	CEBP	Jun-AP1	Atf4	Jun-AP1
9	GRE	Bach2	Atf4	Bach2	RUNX-AML	Bach2	RUNX-AML	Bach2	NF1	Bach2	GRE	Bach2
10	EBF	MafK	NF1	MafK	TEAD2	MafK	CEBP:AP1	Bach1	CEBP:AP1	Bach1	ARE	Bach1

3.3. Functional enrichment analysis of genes identified by ATAC-seq

The biological process (BP) analysis in GO showed that genes associated with accessible chromatin regions were most enriched in the “phosphorylation”, “metabolic process”, and “protein transport” categories. This was found in all groups and indicates the importance of

maintaining basic cellular functions (Supplementary Table 2). The top BP terms from the GO analysis are shown in Figure 2. In adipogenic differentiation, four BPs including “cell adhesion”, “angiogenesis”, “extracellular matrix organization”, and “positive regulation of GTPase activity” were consistently up-regulated in each group. In comparison, during osteogenic differentiation, three BPs including “positive regulation of GTPase activity”, “positive regulation of Rho GTPase activity”, and “extracellular matrix organization” were consistently up-regulated in each group. Interestingly, whether during adipogenic or osteogenic differentiation, the function of the top-ranking up-regulated genes on the seventh day was significantly different from that on the third and fifth days.

The genes associated with accessible chromatin regions were then subjected to KEGG pathway analysis. The top 10 pathway terms in each group are listed Supplementary Table 3. The major pathways identified in each group included “cancer”, “regulation of actin cytoskeleton”, “proteoglycans in cancer”, “focal adhesion”, and “insulin signaling pathway”. The top 10 pathways that showed changes in the differentiated cells and MSCs are seen in Figure 3. Five pathways were consistently up-regulated in adipogenic differentiation, including “Rap1 signaling pathway”, “pathways in cancer”, “adherens junction”, “protein digestion and absorption”, and “PI3K-Akt signaling pathway”. On the other hand, three pathways were consistently up-regulated during osteogenic differentiation, including “Rap1 signaling pathway”, “focal adhesion”, and “cGMP-PKG signaling pathway”.

3.4. RNA-seq Results

RNA-seq was performed on the same batches of cells as ATAC-seq, and no significant differences were observed in the numbers of genes identified in each group (Table 1). Using log2fc > 1 or < - 1, FDR < 0.05 as the screening criteria, genes showing significantly different expression were screened out; these are shown in Table 3 and Figure 4. We observed that there was more variation in the numbers of genes during adipogenesis than during osteogenesis. The differentially expressed genes identified by RNA-seq were then analyzed by GO and KEGG, and histograms of the enriched categories are shown in Supplementary Figure 3 and Supplementary Figure 4. Unexpectedly, the enriched BPs and pathways seen in RNA-seq were quite different from those seen in ATAC-seq. For example, the “fatty acid metabolism” and “adipocytokine signaling pathway” pathways were significantly up-regulated in RNA-seq but not in ATAC-seq during adipogenic differentiation. Similarly, “Rap1 signaling pathway” and “focal adhesion” were significantly up-regulated in ATAC-seq but not in RNA-seq during osteogenic differentiation.

Table 3
Comparison of the numbers of differentially expressed genes between groups during the early stage of osteogenic/adipogenic differentiation

Comparison	Down Gene Num.*	Up Gene Num.*
AD3 *vs.* MSC	1305	1454
AD5 *vs.* MSC	1723	1308
AD7 *vs.* MSC	1763	1581
OB3 *vs.* MSC	1162	720
OB5 *vs.* MSC	1214	698
OB7 *vs.* MSC	1087	1016

*The screening criteria for differentially expressed genes were log2fc > 1 or < - 1, FDR < 0.05

Down, downregulated

Up, upregulated

3.5. Combined ATAC-seq and RNA-seq analysis

The number of overlapped genes between ATAC-seq and RNA-seq for the different groups are shown in Figure 5. In terms of proportion, overlapping genes accounted for only a small proportion of the genes identified by ATAC-seq but a higher proportion of the total genes from RNA-seq.

The top 10 BP terms from GO analysis of the overlapping genes are shown in Supplementary Figure 5. During adipogenic differentiation, “small molecule metabolic process” and “lipid metabolic process” were significantly up-regulated in the AD3 and AD5 groups. In osteogenic differentiation, in contrast, considerable variation was observed in the top 10 enriched BPs, with “extracellular matrix organization” being the only BP which was significantly up-regulated in each group.

The overlapping genes were also subjected to KEGG pathway analysis. The top 10 BP terms in each group are shown in Supplementary Figure 6. In adipogenic differentiation, “PPAR signaling pathway” and “fatty acid metabolism” were significantly up-regulated in the AD3 and AD5 groups while, during osteogenic differentiation, “TGF-beta signaling pathway” and “focal adhesion” were significantly up-regulated in the AD3 and AD5 groups.

3.6. PCR verification

We randomly selected 12 genes from the overlapped genes for qRT-PCR verification which showed that the expression of these representative genes was completely consistent with the RNA-seq data, indicating the reliability of the sequencing results (Figure 6).

4. Discussion

Differentiation of MSCs into adipocytes or osteoblasts is a complex process. During each process, the MSCs are required to undergo lineage commitment stage and cellular maturation, accompanied by substantial alterations in gene expression [16]. However, the mechanisms of transcriptional activation of key genes are still unknown. Therefore, we have attempted to describe the chromatin regional landscape in combination with gene transcription at the early stages after induction for an in-depth understanding of the regulatory mechanisms involved in MSC differentiation.

ATAC-seq technology differs from RNA-seq in that it can provide information on accessible chromatin regions at a genome-wide level and at specific times, allowing the effective detection of patterns in transcriptional activation under specific conditions. ATAC-seq has been applied to the investigation of numerous complex diseases, including cutaneous T cell lymphoma [17] and diabetes [18], amongst others. ATAC-seq has also been used in MSCs to identify cellular diversity from different tissue origins [19] and has also been used to study the chromatin architecture in epidermal MSCs [20]. In contrast to these earlier studies, we focused on changes in chromosome accessibility during the directional differentiation of MSCs. The sequencing data showed that cultured MSCs have more than a hundred thousand accessible chromatin regions, mainly concentrated near the transcription starting point, and consistent with previously published ATAC-seq data on MSCs [19]. However, due to the differences in growth environments *in vitro* and *in vivo*, our results cannot yet predict the accessible chromatin conditions in MSCs *in vivo*.

We observed that chromatin accessibility changes dynamically during MSC differentiation. This is the result not only of external stimulation but also caused by alternations in gene expression. Interestingly, the numbers of expressed genes identified by RNA-seq did not change significantly between time points, while significant fluctuation was seen in the ATAC-seq data. Clearly, these low numbers do not imply that the type of gene expression in each group is fixed, as numerous studies have shown significant changes in gene expression during MSC differentiation [21, 22]. A recent study proposed that chromatin accessibility is a more accurate means for identifying cell types than transcriptome analysis [19]. Our results show that overlapping genes between the ATAC-seq and RNA-seq data only accounts for a small part of the enriched genes identified by ATAC-seq, indicating that changes in chromatin accessibility do not correspond perfectly with changes in gene expression. These complex cytological functions require further exploration.

A useful feature of ATAC-seq is that it reveals transcription factor-binding motifs under physiological conditions [23]. At specific stages, we observed that the main motifs identified in each group were members of the bZIP family, suggesting that bZIP family members play important roles in maintaining basic cellular functions [24]. However, the identification of differentially enriched motifs is more meaningful for the study of transcription factors at different time-points during the differentiation process. During adipogenic and osteogenic differentiation, the CREB motif was the most significantly up-regulated motif in the AD3 and AD5 groups, highlighting its importance during adipogenesis [25]. In addition to CREB, NFIL3 and HLF were also significantly up-regulated in the AD3 and AD5 groups. The bZIP transcription factor NFIL3, also known as E4BP4, regulates a variety of physiological processes ranging from viability to the circadian rhythm [26]. Recently, NFIL3 was found to be significantly up-regulated during adipogenesis and to mediate glucocorticoid-regulated adipogenesis [27]. HLF is also a member of the bZIP transcription factor family [28] and is believed to participate in the physiological regulation of cellular lipid levels [29]. The precise roles of NFIL3 and HLF in adipogenesis are worthy of further study. During osteogenesis, the TEAD and RUNX families were observed to be the most significant up-regulated motifs in the first five days. Compared with the RUNX family of transcription factors, the role of the TEAD family in osteogenic differentiation has been less studied. TEAD family members contain a strongly conserved DNA-binding domain, the TEA domain [30]. Recently, TEAD2 was identified as a novel regulator of osteogenesis [31], indicating the potential role of the TEAD family in the regulation of the osteogenic process. We noticed that the up-regulated motifs enriched on the seventh day were quite different compared with those observed on the fifth and third days, during both adipogenic and osteogenic differentiation. However, the underlying mechanism is unclear. Interestingly, CREB, NFIL3, and HLF, all of which were up-regulated in the first five days of adipogenic differentiation, were only up-regulated in the OB7 group during osteogenesis; correspondingly, TEADs and RUNX2, which were up-regulated in the first five days of the osteogenic process, were only activated in the AD7 group in adipogenesis, suggesting a balanced regulation between the processes of adipogenic and osteogenic differentiation [32].

Functional enrichment analysis is a method to identify classes of genes, which helps to better understand the potential biological processes in gene sets. We observed that the enriched genes from both ATAC-seq and RNA-seq showed clear differences in terms of BP and pathway analyses, indicating different applications between ATAC-seq and RNA-seq. The overlap of genes between the ATAC-seq and RNA-seq data indicates

common features of biological function between the two datasets. For example, during adipogenic differentiation, both ATAC-seq and RNA-seq showed increased enrichment of the PPAR pathway and fatty acid metabolism, both of which are related to adipogenesis. In parallel, up-regulation of the TGF-beta and focal adhesion pathways demonstrate synergism between chromatin structure and gene expression during osteogenic differentiation. There were also some identified overlapping BPs and pathways that are seemingly unrelated to MSC differentiation, and these warrant further study.

In summary, we used ATAC-seq to describe and analyze chromosomal accessibility and gene expression in MSCs during adipogenic/osteogenic differentiation. This work will help to reveal the network of gene loci and transcription factors in cell differentiation and provide more evidence for understanding the changes of epigenetic programming in MSC cells.

Declarations

Author Contributions

Jianjun Xiong contributed to conception, design and writing; Jianyun Liu and Lijun Gan contributed to primary cell culture; Baichen Ma and Huiming Li performed data analysis; Shan He performed qPCR; Ping Wu performed oil red O staining and staining. All of the authors reviewed the manuscript before submission and approved the final manuscript.

Declaration of competing interest

The authors have no conflicts of interest to declare.

Acknowledgements

This work was supported by the National Natural Science Foundation of China (81860165 and 81860796). The authors would like to thank all the reviewers who participated in the review and MJEditor (www.mjeditor.com) for its linguistic assistance during the preparation of this manuscript.

Data sharing statement

Sequencing data of RNA-Seq in this study can be found with accession number of GSE174794 (https://www.ncbi.nlm.nih.gov/geo/query/acc.cgi?acc = GSE174794) in the GEO database at NCBI. Sequencing data of ATAC-Seq are available from the corresponding author on reasonable request.

Institutional Review Board Statement

The study was conducted according to the guidelines of the Declaration of Helsinki, and approved by the Ethics Committee of Affiliated Hospital of Jiujiang University.

Informed Consent Statement

Written informed consent has been obtained from the bone marrow donors to publish this paper

References

1. Kanis JA, Melton LJ, 3rd, Christiansen C, Johnston CC, Khaltaev N: **The diagnosis of osteoporosis**. *Journal of bone and mineral research : the official journal of the American Society for Bone and Mineral Research* 1994, **9**(8):1137-1141.
2. Matsuo K, Irie N: **Osteoclast-osteoblast communication**. *Archives of biochemistry and biophysics* 2008, **473**(2):201-209.
3. Justesen J, Stenderup K, Ebbesen EN, Mosekilde L, Steiniche T, Kassem M: **Adipocyte tissue volume in bone marrow is increased with aging and in patients with osteoporosis**. *Biogerontology* 2001, **2**(3):165-171.
4. Qiu W, Andersen TE, Bollerslev J, Mandrup S, Abdallah BM, Kassem M: **Patients with high bone mass phenotype exhibit enhanced osteoblast differentiation and inhibition of adipogenesis of human mesenchymal stem cells**. *Journal of bone and mineral research : the official journal of the American Society for Bone and Mineral Research* 2007, **22**(11):1720-1731.
5. Pittenger MF, Mackay AM, Beck SC, Jaiswal RK, Douglas R, Mosca JD, Moorman MA, Simonetti DW, Craig S, Marshak DR: **Multilineage potential of adult human mesenchymal stem cells**. *Science (New York, NY)* 1999, **284**(5411):143-147.
6. Janderová L, McNeil M, Murrell AN, Mynatt RL, Smith SR: **Human mesenchymal stem cells as an in vitro model for human adipogenesis**. *Obesity research* 2003, **11**(1):65-74.
7. Bruder SP, Jaiswal N, Haynesworth SE: **Growth kinetics, self-renewal, and the osteogenic potential of purified human mesenchymal stem cells during extensive subcultivation and following cryopreservation**. *Journal of cellular biochemistry* 1997, **64**(2):278-294.

8. Casado-Díaz A, Anter J, Müller S, Winter P, Quesada-Gómez JM, Dorado G: **Transcriptomic Analyses of Adipocyte Differentiation From Human Mesenchymal Stromal-Cells (MSC)**. *Journal of cellular physiology* 2017, **232**(4):771-784.
9. Sun W, Yu Z, Yang S, Jiang C, Kou Y, Xiao L, Tang S, Zhu T: **A Transcriptomic Analysis Reveals Novel Patterns of Gene Expression During 3T3-L1 Adipocyte Differentiation**. *Frontiers in molecular biosciences* 2020, **7**:564339.
10. Piek E, Sleumer LS, van Someren EP, Heuver L, de Haan JR, de Grijs I, Gilissen C, Hendriks JM, van Ravestein-van Os RI, Bauerschmidt S *et al*: **Osteo-transcriptomics of human mesenchymal stem cells: accelerated gene expression and osteoblast differentiation induced by vitamin D reveals c-MYC as an enhancer of BMP2-induced osteogenesis**. *Bone* 2010, **46**(3):613-627.
11. Hurson CJ, Butler JS, Keating DT, Murray DW, Sadlier DM, O'Byrne JM, Doran PP: **Gene expression analysis in human osteoblasts exposed to dexamethasone identifies altered developmental pathways as putative drivers of osteoporosis**. *BMC musculoskeletal disorders* 2007, **8**:12.
12. Kelsey G, Stegle O, Reik W: **Single-cell epigenomics: Recording the past and predicting the future**. *Science (New York, NY)* 2017, **358**(6359):69-75.
13. Buenrostro JD, Giresi PG, Zaba LC, Chang HY, Greenleaf WJ: **Transposition of native chromatin for fast and sensitive epigenomic profiling of open chromatin, DNA-binding proteins and nucleosome position**. *Nature methods* 2013, **10**(12):1213-1218.
14. Corces MR, Buenrostro JD, Wu B, Greenside PG, Chan SM, Koenig JL, Snyder MP, Pritchard JK, Kundaje A, Greenleaf WJ *et al*: **Lineage-specific and single-cell chromatin accessibility charts human hematopoiesis and leukemia evolution**. *Nature genetics* 2016, **48**(10):1193-1203.
15. Yi X, Liu J, Wu P, Gong Y, Xu X, Li W: **The whole transcriptional profiling of cellular metabolism during adipogenesis from hMSCs**. *Journal of cellular physiology* 2020, **235**(1):349-363.
16. Bowers RR, Lane MD: **A role for bone morphogenetic protein-4 in adipocyte development**. *Cell Cycle* 2007, **6**(4):385-389.
17. Qu K, Zaba LC, Satpathy AT, Giresi PG, Li R, Jin Y, Armstrong R, Jin C, Schmitt N, Rahbar Z *et al*: **Chromatin Accessibility Landscape of Cutaneous T Cell Lymphoma and Dynamic Response to HDAC Inhibitors**. *Cancer cell* 2017, **32**(1):27-41.e24.
18. Ackermann AM, Wang Z, Schug J, Naji A, Kaestner KH: **Integration of ATAC-seq and RNA-seq identifies human alpha cell and beta cell signature genes**. *Molecular metabolism* 2016, **5**(3):233-244.
19. Ho YT, Shimbo T, Wijaya E, Ouchi Y, Takaki E, Yamamoto R, Kikuchi Y, Kaneda Y, Tamai K: **Chromatin accessibility identifies diversity in mesenchymal stem cells from different tissue origins**. *Scientific reports* 2018, **8**(1):17765.
20. Lucciola R, Vrljicak P, Gurung S, Filby C, Darzi S, Muter J, Ott S, Brosens JJ, Gargett CE: **Impact of Sustained Transforming Growth Factor-β Receptor Inhibition on Chromatin Accessibility and Gene Expression in Cultured Human Endometrial MSC**. *Frontiers in cell and developmental biology* 2020, **8**:567610.
21. Jiang H, Hong T, Wang T, Wang X, Cao L, Xu X, Zheng M: **Gene expression profiling of human bone marrow mesenchymal stem cells during osteogenic differentiation**. *Journal of cellular physiology* 2019, **234**(5):7070-7077.
22. Huang W, Yang S, Shao J, Li YP: **Signaling and transcriptional regulation in osteoblast commitment and differentiation**. *Frontiers in bioscience : a journal and virtual library* 2007, **12**:3068-3092.
23. Buenrostro JD, Wu B, Chang HY, Greenleaf WJ: **ATAC-seq: A Method for Assaying Chromatin Accessibility Genome-Wide**. *Current protocols in molecular biology* 2015, **109**:21.29.21-21.29.29.
24. Amoutzias GD, Veron AS, Weiner J, 3rd, Robinson-Rechavi M, Bornberg-Bauer E, Oliver SG, Robertson DL: **One billion years of bZIP transcription factor evolution: conservation and change in dimerization and DNA-binding site specificity**. *Molecular biology and evolution* 2007, **24**(3):827-835.
25. Reusch JE, Colton LA, Klemm DJ: **CREB activation induces adipogenesis in 3T3-L1 cells**. *Molecular and cellular biology* 2000, **20**(3):1008-1020.
26. Keniry M, Dearth RK, Persans M, Parsons R: **New Frontiers for the NFIL3 bZIP Transcription Factor in Cancer, Metabolism and Beyond**. *Discoveries (Craiova, Romania)* 2014, **2**(2):e15.
27. Yang Y, Wei H, Song T, Cai A, Zhou Y, Peng J, Jiang S, Peng J: **E4BP4 mediates glucocorticoid-regulated adipogenesis through COX2**. *Molecular and cellular endocrinology* 2017, **450**:43-53.
28. Hunger SP, Ohyashiki K, Toyama K, Cleary ML: **Hlf, a novel hepatic bZIP protein, shows altered DNA-binding properties following fusion to E2A in t(17;19) acute lymphoblastic leukemia**. *Genes & development* 1992, **6**(9):1608-1620.
29. Dzitoyeva S, Manev H: **Reduction of Cellular Lipid Content by a Knockdown of Drosophila PDP1 γ and Mammalian Hepatic Leukemia Factor**. *Journal of lipids* 2013, **2013**:297932.
30. Hwang JJ, Chambon P, Davidson I: **Characterization of the transcription activation function and the DNA binding domain of transcriptional enhancer factor-1**. *The EMBO journal* 1993, **12**(6):2337-2348.
31. Håkelien AM, Bryne JC, Harstad KG, Lorenz S, Paulsen J, Sun J, Mikkelsen TS, Myklebost O, Meza-Zepeda LA: **The regulatory landscape of osteogenic differentiation**. *Stem cells (Dayton, Ohio)* 2014, **32**(10):2780-2793.
32. Moerman EJ, Teng K, Lipschitz DA, Lecka-Czernik B: **Aging activates adipogenic and suppresses osteogenic programs in mesenchymal marrow stroma/stem cells: the role of PPAR-gamma2 transcription factor and TGF-beta/BMP signaling pathways**. *Aging cell* 2004, **3**(6):379-

389.

Figures

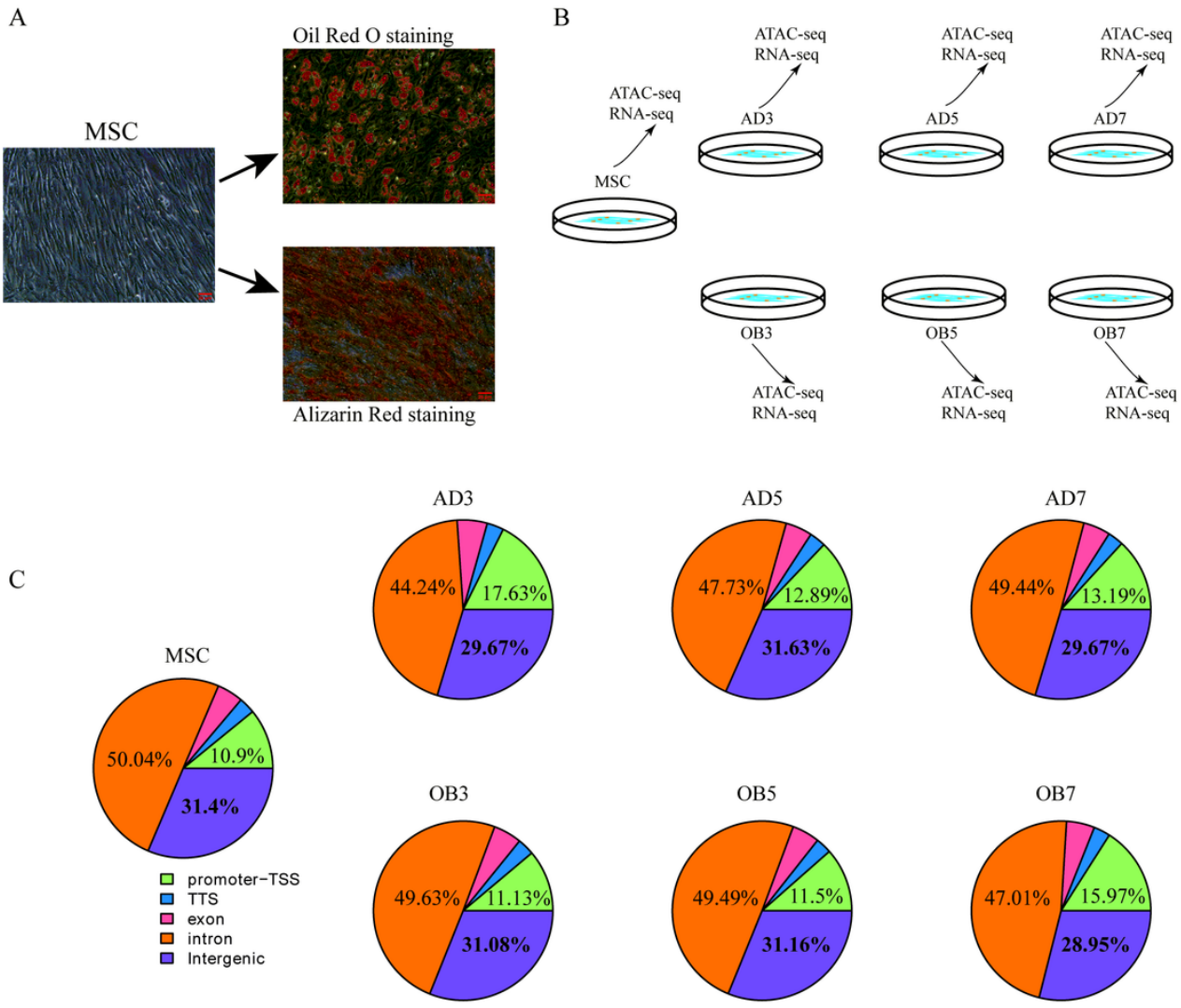

Figure 1

ATAC sequencing analysis of adipogenic and osteogenic differentiation of MSCs. A. Adipogenic and osteogenic differentiation of MSCs demonstrated by Oil Red O and Alizarin Red staining, respectively, on day 14; B. Cell group pattern diagram; C. Peak distributions in the functional regions of the genome shown by statistical analysis.

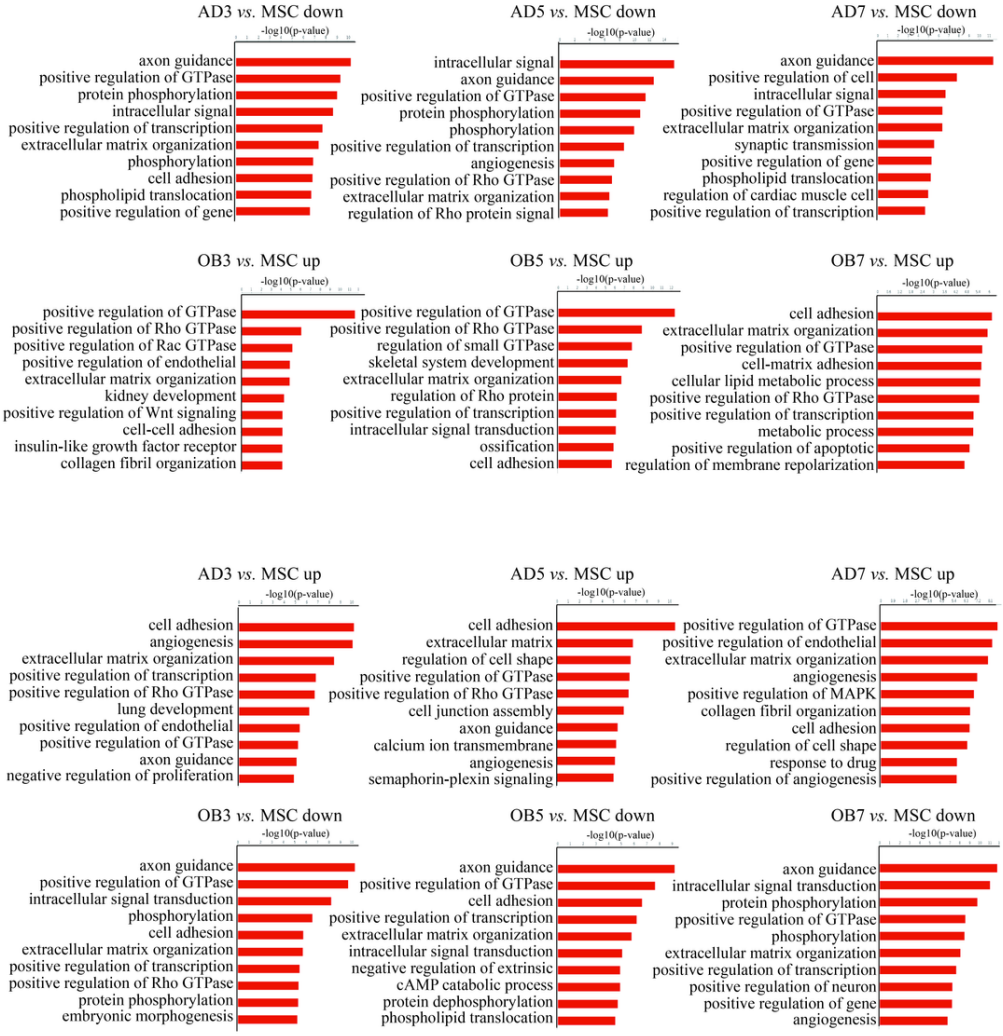

Figure 2

Gene Ontology analysis of genes associated with differences in accessible chromatin regions.

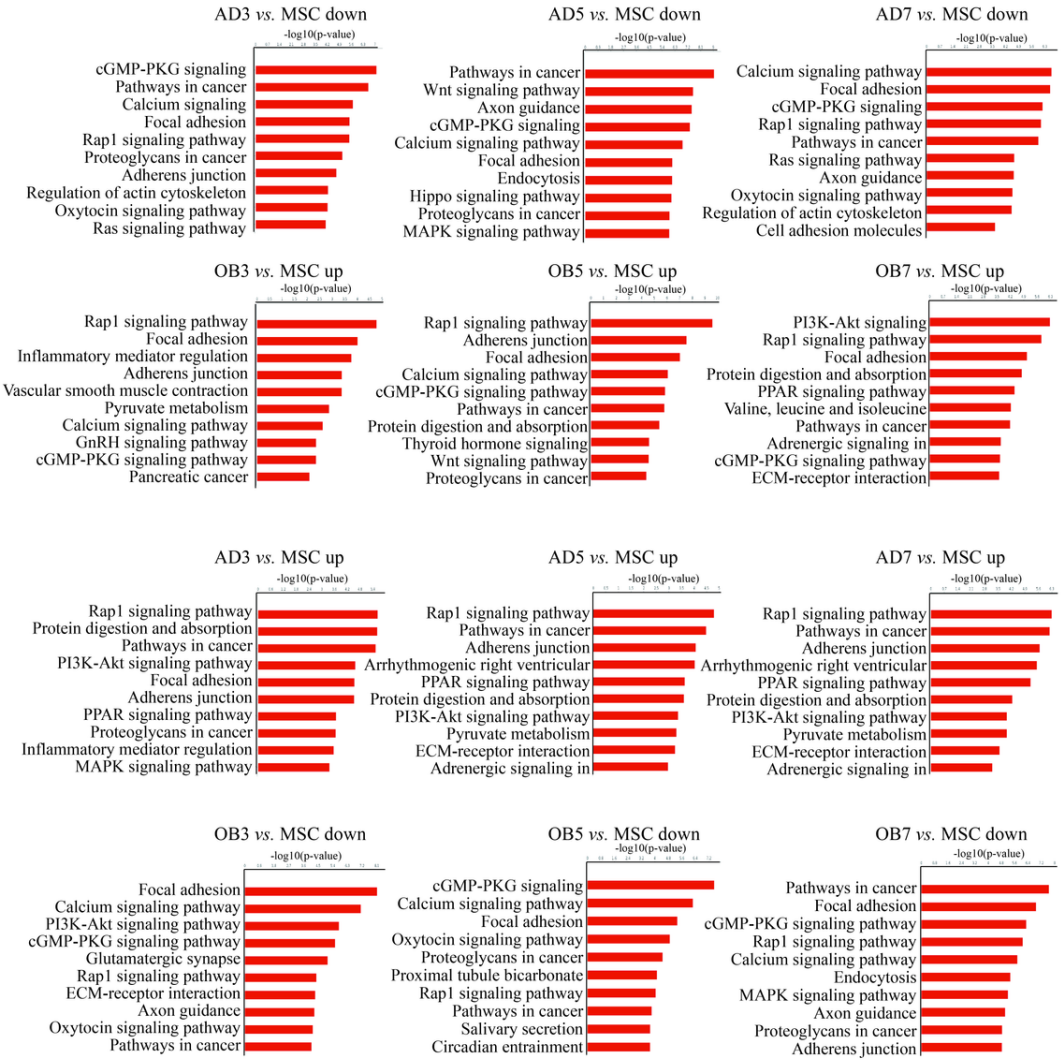

Figure 3

KEGG pathway analysis of genes associated with differences in accessible chromatin regions.

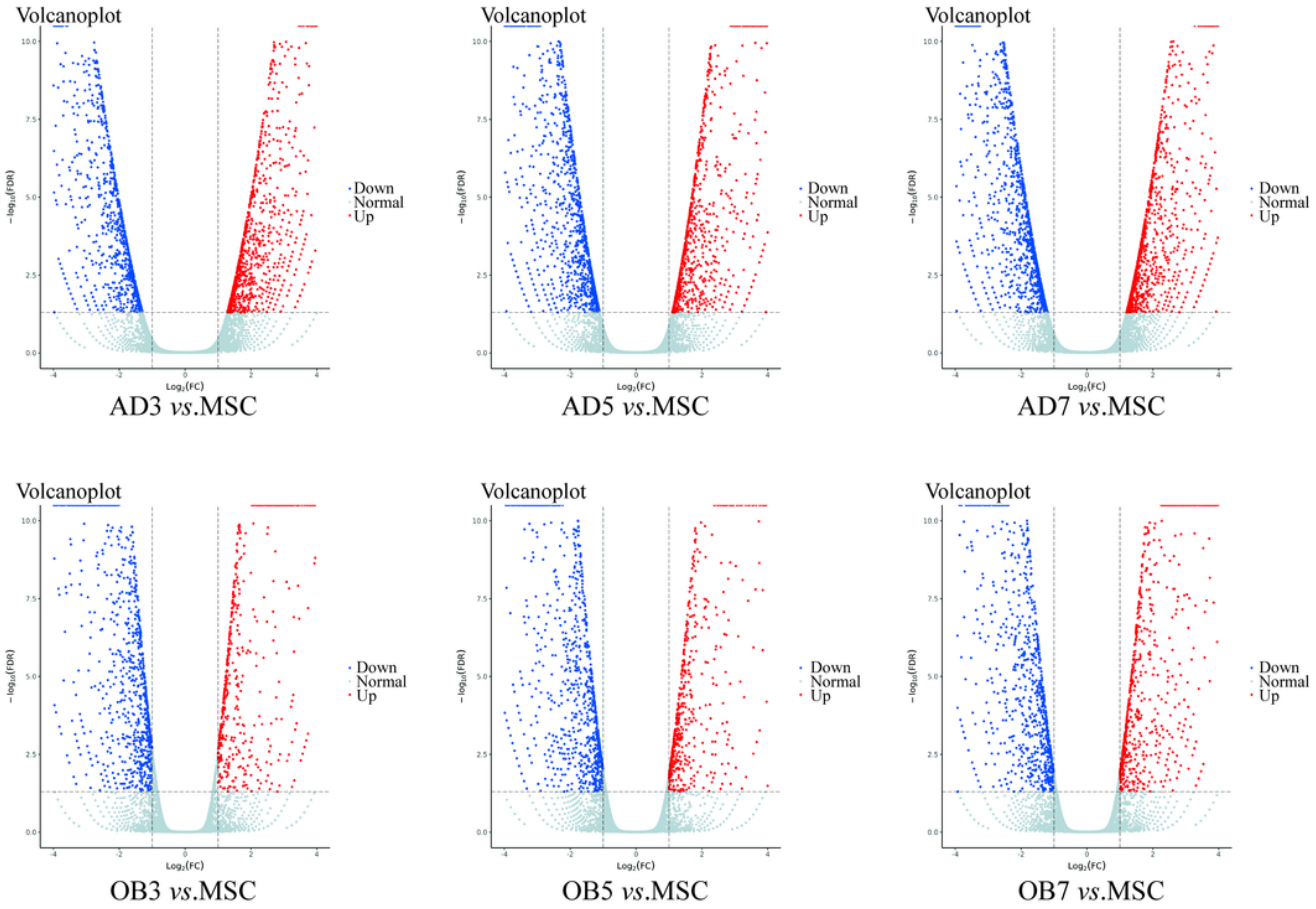

Figure 4

Differentially expressed genes according to group, identified by RNA-seq.

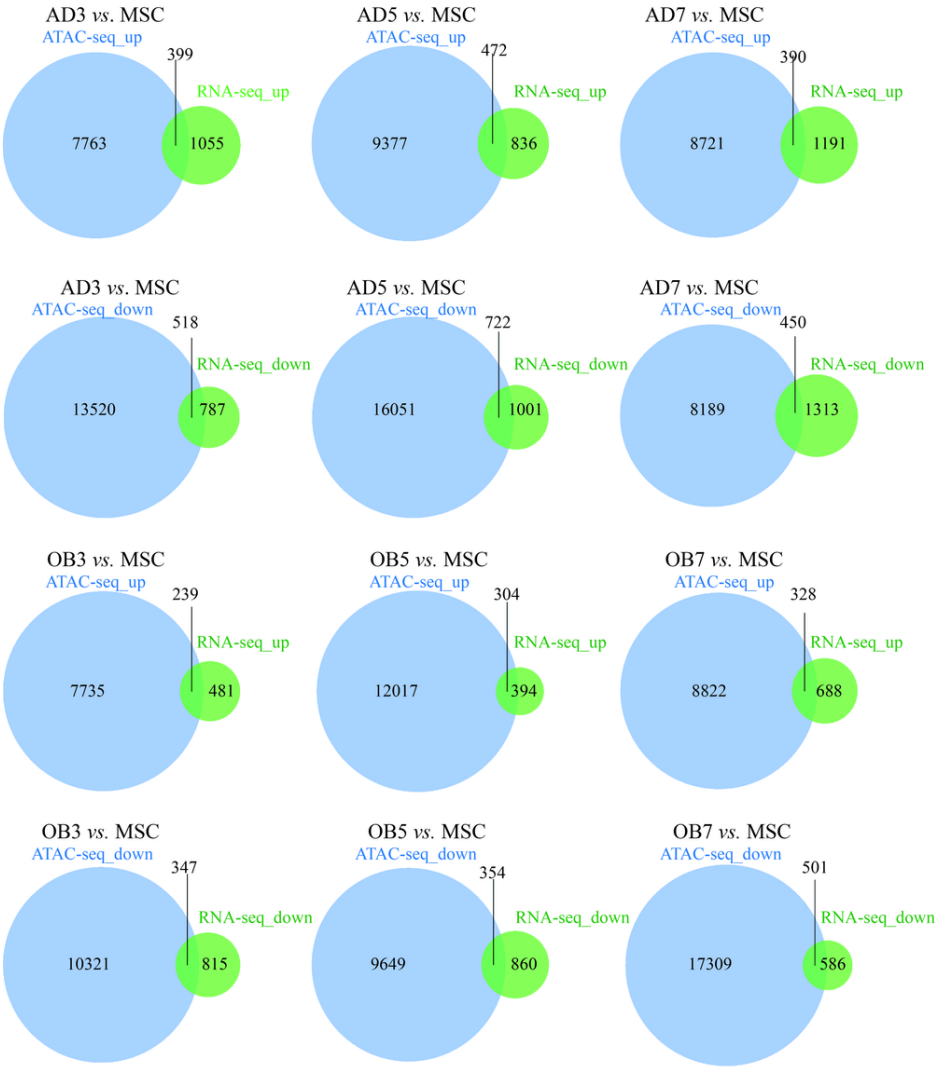

Figure 5

Overlapping of ATAC-seq and RNA-seq data, showing genes common to both datasets.

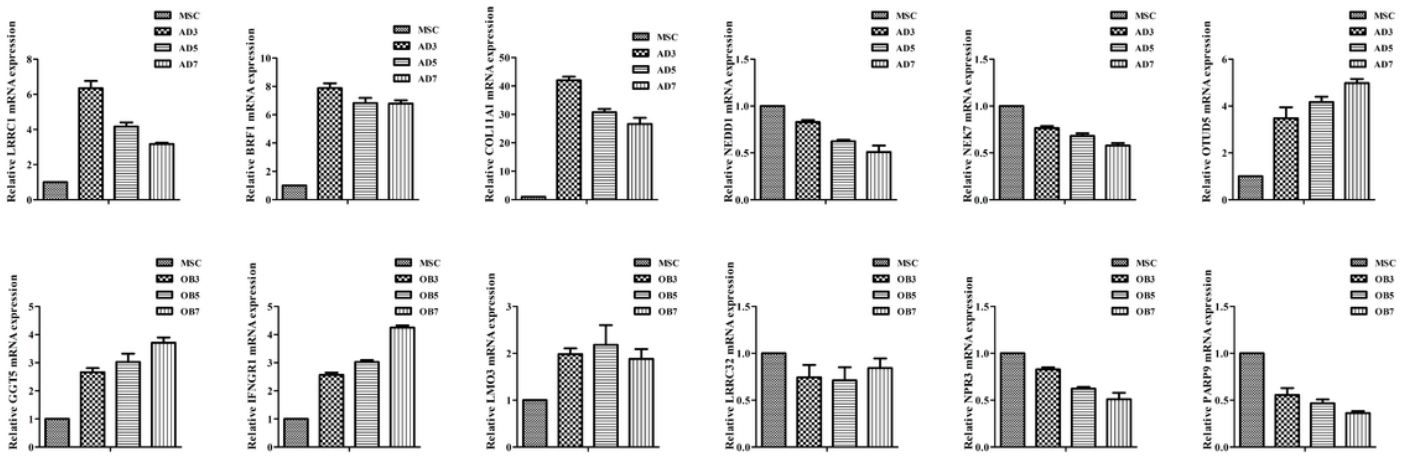

Figure 6

RT-PCR verification of 16 genes identified by RNA-seq.

Supplementary Files

This is a list of supplementary files associated with this preprint. Click to download.

- SupplFig1.tif
- SupplFig2.tif
- SupplFig3.tif
- SupplFig4.tif
- SupplFig5.tif
- SupplFig6.tif
- SupplTable1.docx
- SupplTable2.docx
- SupplTable3.docx
- SupplTable4.docx